


# Organometallic Phyllosilicate-Gold Nanocomplex: An Effective Oral Delivery System of Methotrexate for Enhanced in vivo Efficacy Against Colorectal Cancer

Rajiv Bajracharya\*, Kshitish Chandra Baral\*, Sang Hoon Lee, Jae Geun Song, Hyo-Kyung Han 

College of Pharmacy, Dongguk University-Seoul, Goyang, Korea

\*These authors contributed equally to this work

Correspondence: Hyo-Kyung Han, College of Pharmacy, Dongguk University-Seoul, Dongguk-ro-32, Ilsan-Donggu, Goyang, Korea, Tel +82-31-961-5217, Fax +82-31-961-5206, Email hkhan@dongguk.edu

**Purpose:** Oral administration, although convenient and preferred for treating colorectal cancer (CRC), faces challenges due to limited CRC-related intestinal positioning and a dense mucus barrier. In the present study, a gold-nanoparticle decorated-organometallic phyllosilicate nanocomposite (AC-Au), with a pH-dependent surface coating, was employed for more effective oral delivery of anticancer drugs to treat CRC.

**Methods:** The organometallic AC-Au was synthesized using the in-situ sol-gel method. Subsequently, methotrexate (MTX) was loaded into AC-Au, and the complex (AC-Au/MTX) was surface-coated with poly (methacrylic acid-co-methyl methacrylate) (1:2), a pH-dependent polymer (E/AC-Au /MTX). The in vitro characteristics of nanoparticles were examined using various analytical methods. In vivo efficacy studies were also conducted using an HCT-116 orthotopic colorectal cancer model.

**Results:** AC-Au emerged as a spherical nanoparticle with a mean size of  $26.5 \pm 0.43$  nm, displaying a positive charge over the pH range of 2–10. Both the uncoated and coated drug-loaded nanocomplexes (AC-Au/MTX and E/AC-Au/MTX) were fabricated with high entrapment efficiency ( $> 80\%$ ). Various analyses, including ultraviolet-visible spectroscopy, X-ray powder diffraction, transmission electron microscopy, and energy dispersive X-ray spectroscopy, confirmed the formation of the nanocomplexes. While AC-Au /MTX achieved rapid and extensive drug release at the pH range of 1.2–7.4, E/AC-Au/MTX exhibited pH-dependent drug release, with approximately 23% at pH 1.2 and 74% at pH 7.4. Relative to free MTX, the AC-Au-based nanocomplex significantly enhanced the cytotoxicity of MTX in HCT-116 cells. Furthermore, orally administered E/AC-Au/MTX significantly improved the anti-tumor activity of MTX in an HCT-116 orthotopic colorectal cancer model, resulting in approximately 60% suppression of tumor mass compared with the positive control.

**Conclusion:** The organometallic AC-Au nanocomplex coated with a pH-dependent polymer has the potential to be an effective colonic drug delivery system of MTX, enhancing in vivo efficacy against colorectal cancer.

**Keywords:** methotrexate, aminoclay, gold nanoparticle, colonic delivery, cytotoxicity

## Introduction

Colorectal cancer (CRC) stands as one of the most prevalent cancers worldwide, showing high mortality rates.<sup>1</sup> Various treatments for CRC—including surgery, chemotherapy, radiotherapy, immunotherapy, and combinations thereof—are utilized, depending on the stage and severity of disease.<sup>2</sup> However, these therapeutic approaches encounter some issues including unpredictable innate and acquired resistance, systemic toxicity, and low target selectivity.<sup>3</sup> Metastasis and recurrence are prevalent in CRC, leading to incomplete eradication.<sup>4</sup> High mortality often stems from incomplete tumor resection in surgery, underscoring the critical role that chemotherapy plays in CRC treatment. Some anticancer drugs

commonly used for CRC includes 5-fluorouracil (5-FU), capecitabine, irinotecan, and oxaliplatin, which may be used alone or in combinations of 2 or 3 of these drugs.<sup>3,4</sup> However, their therapeutic success is limited, requiring new therapeutic approaches and technologies to improve the current CRC chemotherapy. Specially, the site-specific delivery of chemotherapeutics should be beneficial to lower adverse effects, enhancing the efficacy of anticancer drugs.<sup>5,6</sup> Furthermore, oral administration of anticancer drugs is convenient and preferred for treating CRC. However, site-selective and oral drug delivery for CRC chemotherapy faces challenges due to limited CRC-related intestinal positioning as well as the dense and viscous mucus barrier in the colorectum, resulting in the limited drug exposure in tumors.<sup>7,8</sup> Therefore, efficient drug delivery to CRC region is critical to improve the efficacy of orally administered anticancer drugs in CRC therapy.

Among the diverse drug carriers available, gold nanoparticles offer shape-related optoelectronic properties, a large surface-to-volume ratio, and biocompatibility, all of which contribute to their potential as drug delivery carriers.<sup>9</sup> Gold nanoparticles also exhibit anticancer activity, providing synergistic effects in chemotherapy,<sup>10</sup> and they are highly amendable to surface coating with various organic/inorganic polymers. Particularly, the surface modification for a wide range of functional ligands expand the application of gold nanoparticles for precise drug targeting and controlled release.<sup>11</sup> In fact, gold nanoparticle-based drug delivery systems have been widely studied for targeting specific cells or tissues.<sup>12,13</sup> For example, Pal et al<sup>14</sup> synthesized the gold nanoparticles modified with plectin-1-targeted multifunctional peptides, demonstrating a highly selective accumulation of these nanoparticles in tumors, without evading into adjacent normal pancreas tissues. In addition, these plectin-1-targeted gold nanoparticles could deliver gemcitabine selectively into the cancer cells, achieving high antitumor efficacy in a PANC-1 orthotopic xenograft model.<sup>14</sup> Diverse surface modification of gold nanoparticles enhances stability, drug-loading capacity, cellular uptake, and target selectivity,<sup>15</sup> reinforcing gold nanoparticles' advantages and high potential for treating malignant tumors. Furthermore, it is applicable for photothermal therapy and bioimaging.<sup>11</sup> Therefore, gold nanoparticles should be a promising drug delivery platform to overcome the limitations of the standard chemotherapy.

Organometallic phyllosilicate clays, such as 3-aminopropyl functionalized magnesium phyllosilicate (aminoclay, AC), are stably dispersed as cationic nano-sheets in aqueous media. They can easily form nanocomplexes with various biomolecules, thereby improving the stability of entrapped biomolecules against environmental stress and facilitating cellular drug uptake.<sup>16–18</sup> AC also exhibits anti-inflammatory effects,<sup>19</sup> a beneficial attribute for CRC treatment, given that CRC often accompanies intestinal inflammation.<sup>20</sup> With its large surface area and controllable surface charge enabling diverse modifications, AC stands as a highly competitive drug delivery carrier. Moreover, AC can stabilize various metal ions<sup>21</sup> and be decorated with gold nanoparticles formed through NaBH<sub>4</sub> reduction, leading to the water-soluble AC-Au nanocomposite.

Owing to the potential therapeutic benefits of gold nanoparticles and AC, the present study employed a gold-nanoparticle decorated-AC nanocomposite (AC-Au), with a pH-dependent surface coating, for more effective oral delivery of anticancer drugs to treat CRC. This pH-responsive AC-Au nanocomplex may enhance CRC therapy by preventing immature drug release in the upper gastrointestinal tract, interacting with the negatively charged mucous layer and prolonging residence time in the colorectum, and increasing cellular drug uptake. Methotrexate (MTX) was chosen as a model drug for this study, and the colonic delivery system of MTX was fabricated using an AC-Au nanocomposite and a pH-dependent methacrylic acid-methyl methacrylate copolymer (1:2). The *in vivo* efficacy of the developed formulation was evaluated in orthotopic CRC-bearing mice.

## Materials and Methods

### Materials

MTX hydrate was procured from Tokyo Chemical Industry Co., Ltd, while chloroauric acid (HAuCl<sub>4</sub>), 3-aminopropyl-trimethoxysilane, and Corning® Matrigel® basement membrane matrix were purchased from Sigma-Aldrich Co. (St Louis, MO, USA). Methacrylic acid-methyl methacrylate copolymer (1:2) (Eudragit®-S 100) was kindly gifted by Evonik Korea Ltd. (Seoul, Korea). Magnesium chloride hexahydrate (98%) and other inorganic salts were sourced

from Junsei Chemical Co., Ltd (Tokyo, Japan), and all other chemicals and solvents were purchased from Merck KGaA (Darmstadt, Germany). All solvents used were high-performance liquid chromatography (HPLC) grade.

Cell culture medium (RPMI-1640), fetal bovine serum (FBS), penicillin–streptomycin, and other reagents for cell culture studies were acquired from GE Healthcare Life Sciences (South Logan, UT, USA). HCT-116 cells (human colorectal adenocarcinoma cells), CCD-18Co (normal human colon cells) and HEK-293 (human embryonic kidney cells) were purchased from the Korean Cell Line Bank (Seoul, Korea) and cultured in RPMI-1640 medium containing 10% FBS and 1% antibiotics at 37 °C, 5% CO<sub>2</sub>, and 90% relative humidity.

## Preparation of AC-Au Nanocomposite

Aminoclay decorated with gold nanoparticles (AC-Au) was synthesized using an in situ sol-gel method as reported previously.<sup>22,23</sup> Briefly, MgCl<sub>2</sub>·6H<sub>2</sub>O (8.26 mmol) was dissolved in 20 mL of 3.8 mM HAuCl<sub>4</sub> solution, followed by the addition of 2 mL of 3-aminopropyltrimethoxysilane. The yellow mixture was stirred overnight at room temperature, then heated at 75 °C for 24 h. The gold nanoparticles' formation via thermal reduction changed the mixture's color to dark red-wine. After centrifugation at 6000 × g for 10 min, the precipitate was washed with ethanol and dried in a vacuum oven at 25 °C for 24 h.<sup>24</sup>

## Preparation of Drug-Loaded Nanoparticles

The AC-Au nanocomposite was dispersed in water under ultra-sonication for 2 min. MTX (5 mg/mL) dissolved in NaOH (0.04 mol/L) was added dropwise to an aqueous dispersion of AC-Au (10 mg/mL) at a weight ratio of MTX to AC-Au of 1:3, stirring at 250 rpm. The mixture was stirred for 24 h and then centrifuged at 9800 × g for 10 min. The resulting precipitate was washed with 0.1 mol/L NaCl and distilled water and then dried in a vacuum oven at 25 °C for 24 h. MTX-loaded AC-Au nanoparticles (AC-Au/MTX) were obtained as fine orange colored-powders.

Subsequently, the obtained AC-Au/MTX nanoparticles underwent the surface coating with a pH-dependent polymer (methacrylic acid-methyl methacrylate copolymer (1:2)). AC-Au/MTX (4 mg) were dispersed in HCl (5 mmol/L, 1 mL) and then added dropwise into 2% methacrylic acid-methyl methacrylate copolymer (1:2) in ethanol (1 mL), stirring at 300 rpm.<sup>25</sup> After 1 h, the mixture was centrifuged at 9800 × g for 10 min. The resulting precipitate was washed with distilled water, and dried in a vacuum oven at 25 °C for 24 h. The surface coated AC-Au/MTX (E/AC-Au/MTX) were obtained as light pink colored powders.

## Structural Characterization of Nanoparticles

The surface plasmon resonance of nanoparticles was monitored using UV/visible spectrophotometry (OPTIZEN POP, Mecasys, Daejeon, Korea). Particle size and zeta potential of nanoparticles were assessed by dynamic light scattering using a Zetasizer Nano-ZS90 (Malvern Instruments, Malvern, UK). The nanoparticles' entrapment efficiency (EE) was calculated as follows (Figure S1):

$$EE (\%) = \frac{\text{Drug amount initially added} - \text{Drug amount in supernatant}}{\text{Drug amount initially added}} \times 100$$

With Fourier-transform infrared spectroscopy (FT-IR; Nicolet™ iS™ 5; Thermo Fisher Scientific, Waltham, MA, USA), the FT-IR spectrum of each sample was obtained over a wavenumber range of 4000–600 cm<sup>-1</sup>. X-ray diffraction (XRD) patterns were examined using an X-ray diffractometer (X'Pert APD, PHILIPS, Amsterdam, The Netherlands), employing CuKα radiation at 40 kV and 30 mA. XRD analysis was performed at the Korea Basic Science Institute (Daegu Center, Korea). The morphology and elemental compositions of the nanoparticles were investigated using transmission electron microscopy (TEM) (JEM-F200; JEOL Ltd., Tokyo, Japan), combined with energy dispersive X-ray (EDX) spectrometer. Both TEM and EDX analyses were conducted at Yonsei University (Seoul, Korea).

## In vitro Drug Release

In vitro drug release characteristics of nanoparticles were examined at pH 1.2 and 7.4. Drug-loaded nanoparticles, equivalent to 1 mg of MTX, were incubated in each dissolution medium at 37 °C while being stirred at 50 rpm. At

predetermined time points, samples were collected, centrifuged at  $9800 \times g$  for 10 min, and drug concentrations in the supernatant were analyzed by HPLC. In addition, the dissolution kinetics of E/AC-Au/MTX were assessed using the different kinetic equations including zero order, first order, Higuchi, and Korsmeyer-Peppas equations as reported previously.<sup>26,27</sup>

The drug release profiles of E/AC-Au/MTX were evaluated after 3 months of storage at both 4 °C and 25 °C. Samples were stored in amber glass vials with tight screw caps at the specified temperatures. After the 3-month storage period, drug release profiles of E/AC-Au/MTX were examined at pH 1.2 and 7.4, as described, and compared to those from Day 0.

## Cytotoxicity Study

The cytotoxicity study was conducted using the MTT (3-[4,5-dimethylthiazole-2-yl]-2,5-diphenyltetrazolium bromide) assay. HCT-116 cells were seeded into 96-well plates at a density of  $1 \times 10^4$  cells per well. After a 24 h-incubation at 37 °C, the medium was removed, and cells were treated with either MTX or MTX-loaded nanoparticles dispersed in the cell culture medium at the different concentrations. Furthermore, the cytotoxic effects of vehicle components (Eudragit®-S 100, AC, and AC-Au) were evaluated in HCT-116 cells over a concentration range of 0.1–1000 µg/mL. Furthermore, the cytotoxicity of vehicle components was evaluated in CCD-18Co cells and HEK-293 cells, to assess the potential toxicity of vehicles in non-cancer cells from different origins. Following a 48 h-incubation period, the medium was removed, and 0.5 mg/mL MTT (100 µL) was added to each well. The plates were incubated at 37 °C for 4 h. Then, 100 µL of dimethyl sulfoxide was added to each well, dissolving the formazan crystals. The absorbance of each sample was measured at 550 nm on a microplate reader (SpectraMax M2e, Molecular Devices, CA, USA), and the  $CC_{50}$  was calculated using non-linear regression analysis in SigmaPlot® (Systat Software Inc., Palo Alto, CA, USA).

## In vivo Efficacy Study in HCT-116 Tumor-Bearing Mice

The in vivo efficacy of E/AC-Au/MTX was assessed in an HCT-116 orthotopic CRC mouse model and compared with MTX. Animal studies adhered to the “Guiding Principles in the Use of Animals in Toxicology” set by the Society of Toxicology (USA), and the study protocol was approved by the review committee of Dongguk University (IACUC-2021-059-1). Male BALB/c nude mice (15–20 g) were sourced from Orient Bio Inc. (Seongnam, Korea) and housed at 21–22 °C with a 12 h light/dark cycle. Prior to the experiments, mice aged 6–8 weeks were randomly divided into five groups ( $n = 4$  per group). To establish the orthotopic CRC model, as previously reported,<sup>28,29</sup> 50 µL of a cell suspension ( $5 \times 10^6$  HCT-116 cells in RPMI-1640 with 50% Matrigel) was injected aseptically into the caecum of each mouse, except for mice in the healthy control group. After 5 days post-injection, HCT-116 tumor-bearing mice were orally administered with phosphate-buffered saline (PBS), empty vehicle (E/AC-Au), free drug (MTX, 2 mg/kg), or MTX-loaded nanoparticles (E/AC-Au/MTX, equivalent to 2 mg/kg of MTX) every other day for 8 weeks. Each formulation was dispersed in PBS. After 8 weeks, mice were sacrificed, and antitumor efficacy was evaluated based on changes in body weight and tumor mass.

## HPLC Assay

MTX concentrations in samples were measured using an HPLC system (Perkin Elmer Shelton, CT, USA) with a reversed-phase chromatographic column (Gemini C18, 4.6×150 mm, 5 µm; Phenomenex, Torrance, CA, USA). The mobile phase (0.1% acetic acid: acetonitrile = 85: 15, v/v) was eluted at a flow rate of 1.0 mL/min at 30 °C, with the UV wavelength set at 290 nm. Folic acid was used as an internal standard, and the MTX calibration curve was linear ( $r^2 = 0.999$ ) over a concentration range of 0.5–100 µg/mL.

## Statistical Analysis

The data are represented as mean values with standard deviation. Statistical analysis was performed using one-way ANOVA followed by Dunnett’s test. A  $p$ -value less than 0.05 was considered a statistically significant difference.

**Table 1** Characteristics of Nanoparticles

Sample	Size (nm)	PDI	ZP (mV)	EE (%)
AC-Au	26.5 ± 0.43	0.29 ± 0.04	21.6 ± 0.84	-
AC-Au/MTX	182 ± 28.2	0.52 ± 0.03	16.2 ± 0.04	90.2 ± 0.69
E/AC-Au/MTX	389 ± 25.3	0.44 ± 0.05	-21.1 ± 3.12	80.2 ± 0.19

## Results and Discussion

### Preparation and Structural Characterization of Nanoparticles

The AC-Au nanocomplex was prepared using an in-situ sol-gel method, displaying a distinct color change upon AC-Au formation. As detailed in Table 1 and Figure S2, AC-Au emerged as positively charged nanoparticles in a narrow size distribution with a mean size of  $26.5 \pm 0.43$  nm. While the aminoclay solution is colorless and optically transparent, the AC-Au suspension exhibits a wine-red color and a characteristic plasmon band at 522 nm (Figure 1A and B). TEM-EDX analysis further confirmed the formation of AC-Au (Figure 1C), revealing its size and spherical shape, which corresponded with the dynamic light scattering results. Additionally, the EDX analysis clearly identified elements from both AC and Au (Figure 1C). AC-Au demonstrated good storage stability, retaining the plasmon band at 522 nm over a 3-month storage period at both 4 °C and 25 °C (Figure 1D).

Subsequently, anticancer drug (MTX)-loaded AC-Au (AC-Au/MTX) was fabricated with high entrapment efficiency (90.2%). The nanocomplex was positively charged, exhibiting a spherical shape and a mean particle size of  $182 \pm 28.2$  nm (Table 1 and Figure S2). The FT-IR spectrum of AC-Au/MTX indicated the characteristic absorption bands from AC-Au and MTX; aminopropyl groups of AC ( $\text{N-H}$ ,  $1609\text{ cm}^{-1}$ ), phyllosilicate framework ( $\text{Si-O-Si}$ ,  $1006\text{ cm}^{-1}$ ;  $\text{Mg-O}$ ,  $550\text{ cm}^{-1}$ ), and amide peaks of MTX ( $1640\text{ cm}^{-1}$  and  $1599\text{ cm}^{-1}$ ) (Figure 2A). In the XRD analysis, AC-Au/MTX showed distinct peaks at  $38.24^\circ$ ,  $44.44^\circ$ ,  $65.07^\circ$ ,  $77.71^\circ$ , and  $81.75^\circ$  from metallic gold, implying that the nanoparticles were of a face centered cubic structure.<sup>30,31</sup> However, the diffraction peaks from crystalline MTX were absent, indicating the amorphous state of MTX in the nanocomplex (Figure 2B). The surface plasmon resonance peaks shifted from 522 nm

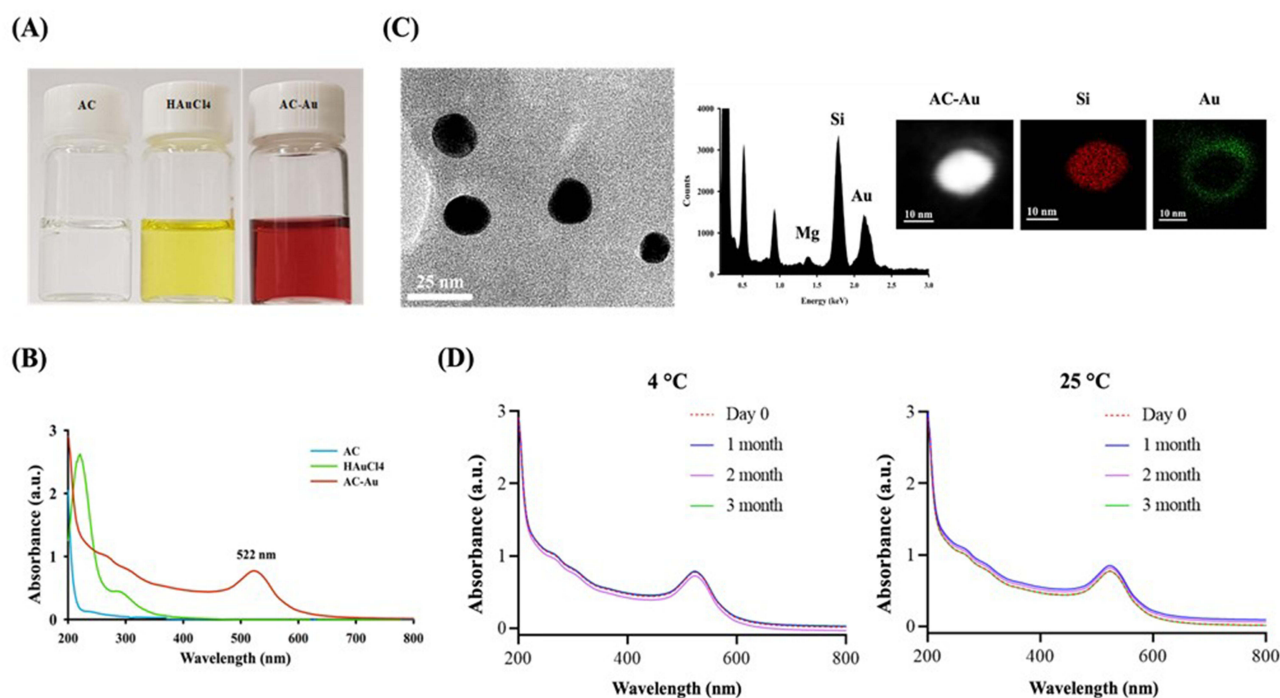


**Figure 1** In vitro characterization of AC-Au nanoparticles. (A) Optical images, (B) UV-visible spectra, (C) TEM-EDX analysis, and (D) Storage stability at both 4 °C and 25 °C.



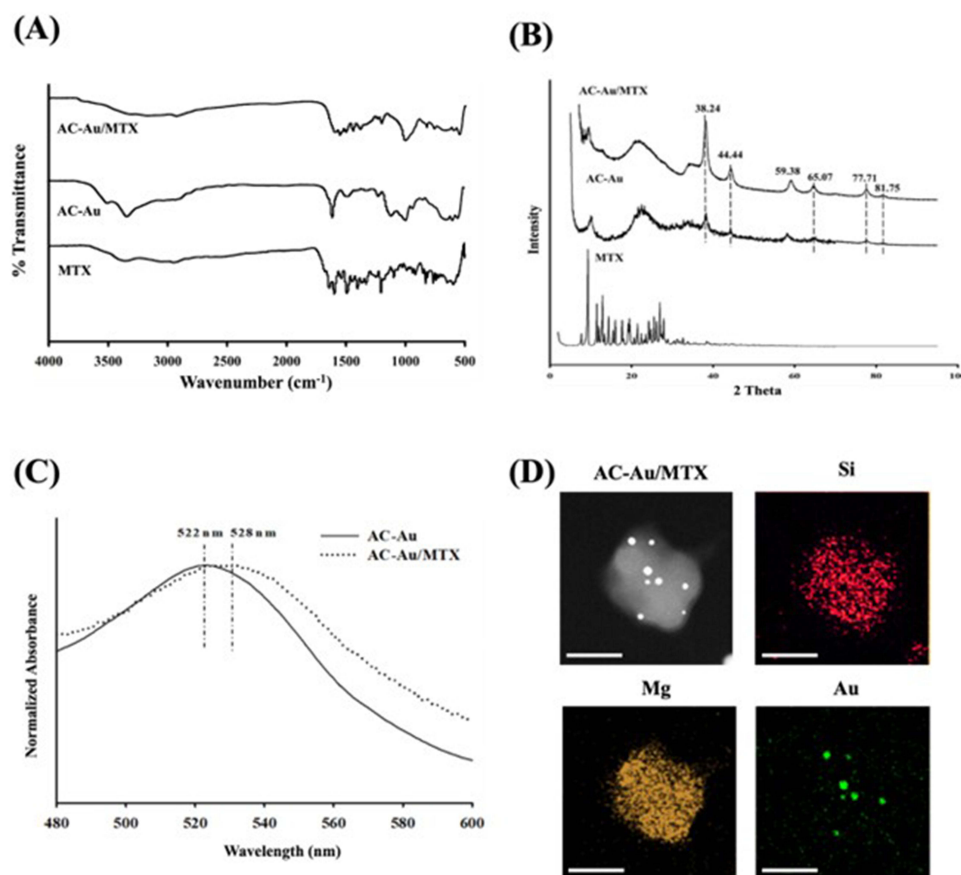


**Figure 2** In vitro characterization of MTX-loaded nanocomplex (AC-Au/MTX). **(A)** FT-IR spectra, **(B)** XRD analysis, **(C)** UV-visible spectra, **(D)** TEM-EDX analysis (Scale bar represents 100 nm).

to 528 nm after drug loading, possibly due to the increased particle size of the drug-loaded nanocomplex (Figure 2C). Additionally, EDX analysis confirmed the distribution of Au throughout the nanocomplex (Figure 2D).

Lastly, to inhibit premature drug release in the stomach and upper intestine, the surface of AC-Au/MTX was coated with poly (methacrylic acid-co-methyl methacrylate) (1:2). This coating increased the particle size and reversed the surface charge from positive to negative, resulting in a coated nanocomplex (E/AC-Au/MTX) with a mean size of  $389 \pm 25.3$  nm and a zeta-potential of  $-21.1 \pm 3.12$  mV (Table 1).

## In vitro Drug Release Study

The in vitro drug release profiles of both uncoated and coated nanoparticles (AC-Au/MTX and E/AC-Au/MTX) were assessed at pH 1.2 and 7.4. At the acidic pH, AC-Au/MTX rapidly released MTX, achieving approximately 84% of drug release within 2 h (Figure 3A). In contrast, E/AC-Au/MTX suppressed the drug release to less than 25% (Figure 3A), suggesting that E/AC-Au/MTX may minimize premature drug release in the stomach. At pH 7.4, both coated and uncoated nanocomplex displayed similar rapid and extensive drug release (approximately 74–78%), likely due to the pH-dependent dissolution of the outer coating layer (Figure 3B). Collectively, these findings indicated that E/AC-Au/MTX could release the entrapped drugs more efficiently in the lower intestine, delivering more anticancer drugs closer to the colonic site. Furthermore, the dissolution kinetics of E/AC-Au/MTX were evaluated by using the different mathematical equations. As shown in Table S1, the in vitro drug release of E/AC-Au/MTX was best fitted to Korsmeyer–Peppas equation, exhibiting good linearity ( $r^2 = 0.9787$ ) and the release exponent ( $n$ ) value of 0.3571. Given that the release exponent ( $n$ ) is within the range of  $0 < n < 0.45$ , the drug release from E/AC-Au/MTX might be controlled by Fickian diffusion process.<sup>27</sup>

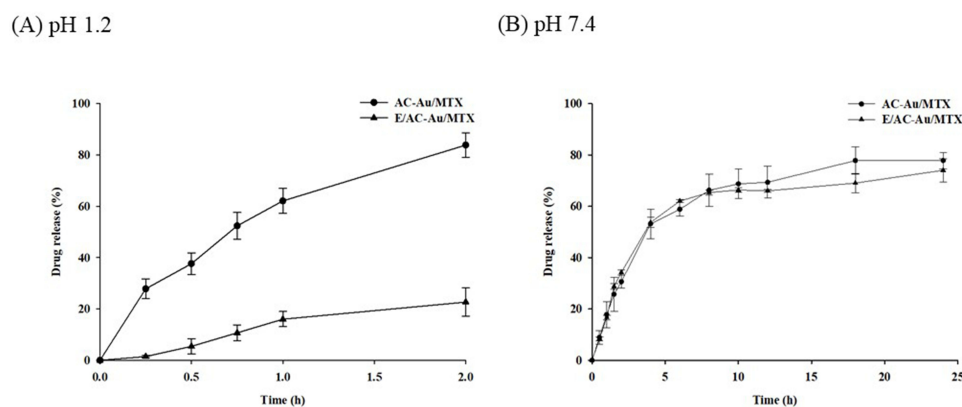


**Figure 3** In vitro drug release profiles of drug-loaded nanocomplex at pH 1.2 (A) and pH 7.4 (B) (mean  $\pm$  SD,  $n=3$ ).

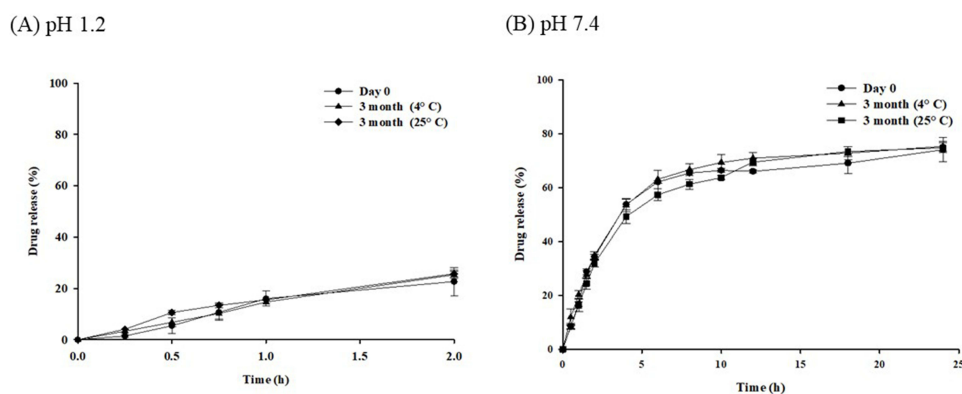


**Figure 4** In vitro drug release profiles of E/AC-Au/MTX after 3-month storage at 4 °C and 25 °C (mean  $\pm$  SD,  $n=3$ ). In vitro drug release studies were performed at pH 1.2 (A) and pH 7.4 (B).

The effect of storage stability on the drug release profiles was evaluated during a 3-month storage period of E/AC-Au/MTX at both 4 °C and 25 °C. As shown in Figure 4, no significant changes in drug release profiles were observed after the 3-month storage at these temperatures, indicating that E/AC-Au/MTX should remain stable under such storage conditions.

## In vitro Cytotoxicity

The cytotoxicity of the drug-loaded nanocomplex was evaluated using the MTT assay in HCT-116 colon cancer cells. As demonstrated in Figure 5A, both AC-Au/MTX and E/AC-Au/MTX substantially enhanced the cytotoxicity of MTX in HCT-116 cells. The  $CC_{50}$  values for AC-Au/MTX and E/AC-Au/MTX were  $0.73 \pm 0.03$  ng/mL and  $0.45 \pm 0.09$  ng/mL, respectively. Considering the  $CC_{50}$  of  $3.09 \pm 0.73$  ng/mL for free MTX, the AC-Au-based nanocomplex increased the cytotoxic activity of MTX by 4.23–6.87 folds, relative to the free drug. These enhanced cytotoxicity of MTX may be explained by several factors. First, AC-Au exhibited significant cytotoxicity in HCT-116 colon cancer cells (Figure 5B), which might contribute to the enhanced toxicity of MTX. Given that AC alone did not affect cell viability even at the concentrations as high as 1000  $\mu$ g/mL (Figure 5B), the cytotoxic effect of AC-Au might be attributed to gold nanoparticles. Given that the cytotoxic effect of nanoparticles is cell type specific, the potential toxicity of AC-Au was also assessed in non-cancer cells from different origins. As illustrated in Figure S3A and S3B, all of vehicle components including AC-Au did not show any significant cytotoxicity in both normal human colon cells and human kidney cells. These results suggest that AC-Au-based nanoparticles can enhance the cytotoxicity of MTX in colon cancer cells with little damage to the normal colonic tissues. In addition, AC-Au-based nanoparticles may enhance paracellular permeability of anticancer drugs, owing to the transient tight junction opening effect of AC.<sup>25,32</sup> Taken together, AC-Au-

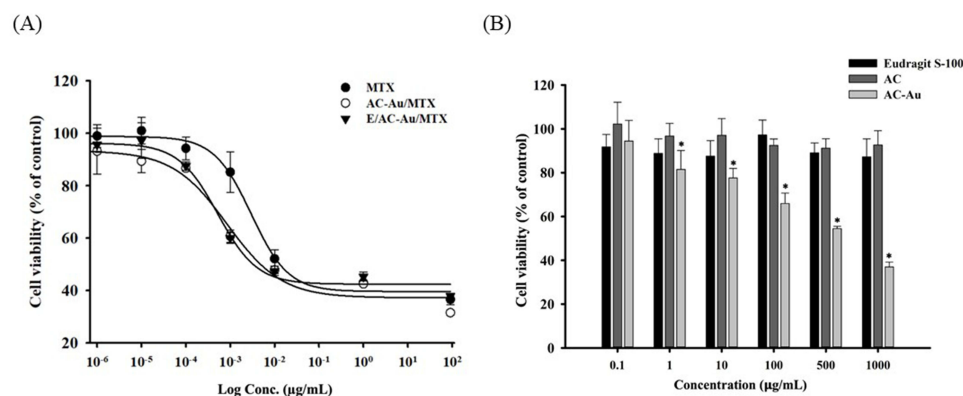


**Figure 5** Cytotoxicity studies in HCT-116 colon cancer cells (mean  $\pm$  SD,  $n = 6$ ). **(A)** Cytotoxic effects of free MTX and MTX-loaded nanoparticles (AC-Au/MTX and E/AC-Au/MTX), **(B)** Cytotoxic effect of vehicle components (a surface coating polymer (methacrylic acid-methyl methacrylate copolymer (1:2) (Eudragit® S 100), AC, and AC-Au). \* $p < 0.05$  compared to the control group.

based drug delivery systems could enhance the cytotoxicity of MTX in colon cancer cells via the combined effect of the improved drug uptake and the cytotoxic effect of AC-Au.

## In vivo Efficacy Study

The antitumor efficacy of E/AC-Au/MTX was examined in mice bearing orthotopic HCT-116 tumors as illustrated in Figure 6A, and the results were compared with those of free MTX, PBS, and empty vehicle. As shown in Figure 6B–D, free MTX minimally inhibited tumor growth, whereas E/AC-Au/MTX significantly suppressed it. In the E/AC-Au/MTX treatment group, the tumor mass was reduced to 565 mg from 1420 mg, representing approximately 60% decrease,

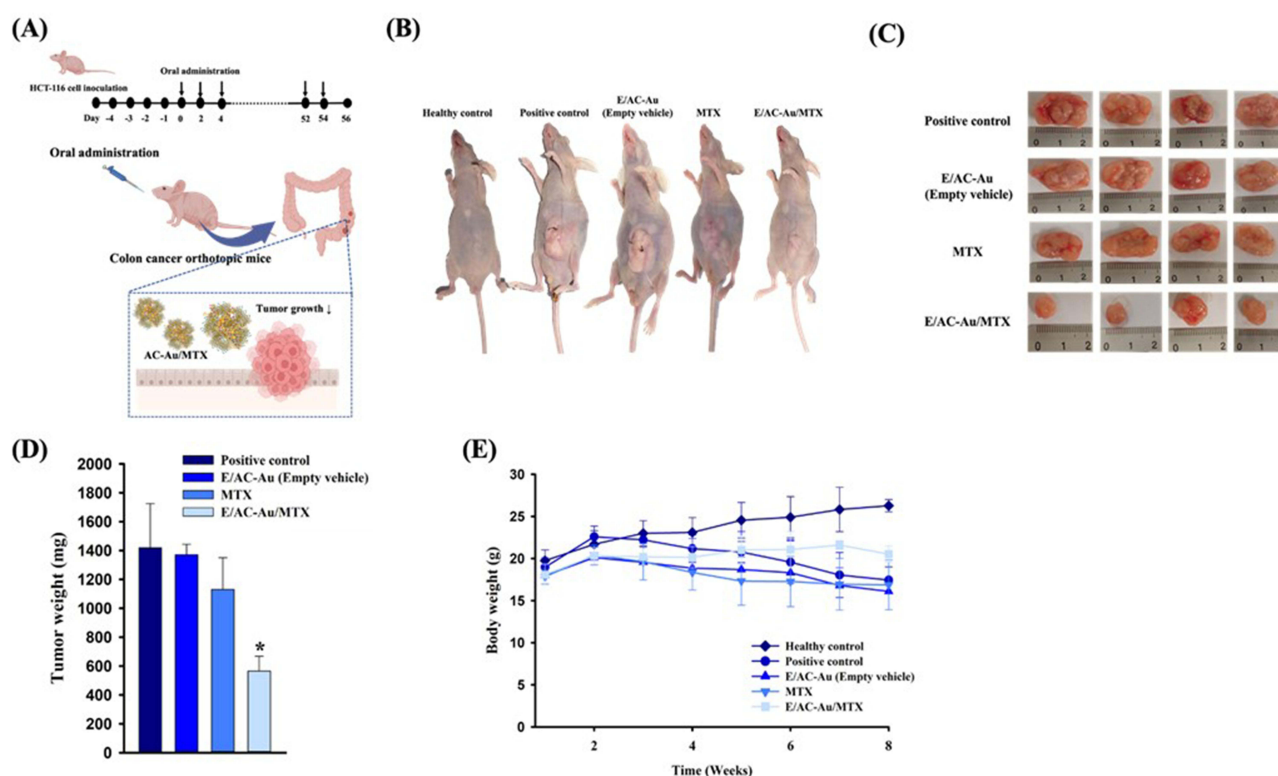


**Figure 6** In vivo efficacy of orally administered E/AC-Au/MTX in HCT-116 orthotopic colorectal cancer mouse model (mean  $\pm$  SD,  $n = 4$ ). **(A)** Illustration of drug treatment in HCT-116 orthotopic colorectal cancer mouse model, **(B)** BALB/c mice after 8-week treatment, **(C)** images of excised tumors after 8-week treatment, **(D)** tumor weight post 8-week treatment, and **(E)** analysis of body weight changes. Dose was equivalent to 2 mg/kg of MTX. \* $p < 0.05$ , denotes significant difference compared with the PBS treatment group (positive control).



compared with the PBS-treated group (Figure 6C and D). The in vivo toxicity was monitored by regularly measuring the body weights of the mice. As depicted in Figure 6E, the E/AC-Au/MTX treatment group maintained body weight without further loss during the 8-week treatment, unlike other treatment groups that displayed dramatic weight loss. The enhanced in vivo efficacy of MTX via E/AC-Au/MTX could be attributable, at least in part, to (i) E/AC-Au/MTX minimizing premature drug release in the upper gastrointestinal tract and increasing drug delivery to the colonic tumor region, and (ii) the dissolution of the outer coating layer at the colonic pH releasing the positively charged AC-Au/MTX nanocomplex, which could interact with the negatively charged mucous layer, prolonging residence time in the colonic region and boosting cellular drug uptake.

In summary, E/AC-Au/MTX appears to be an effective colonic drug delivery system, enhancing the anticancer activity of MTX against the colorectal cancer.

## Conclusion

In this study, the creation of a pH-sensitive E/AC-Au/MTX nanocomplex represented an effective approach to CRC therapy through targeted colonic delivery of MTX. E/AC-Au/MTX was successfully fabricated with high entrapment efficiency, demonstrating excellent storage stability at room temperature. The study highlighted the pH-dependent drug release properties of E/AC-Au/MTX, which favors drug release at pH 7.4, aligning with the pH conditions of the targeted lower intestinal region. Dissolution kinetics was well fitted to Korsmeyer-Peppas equation, implying the Fickian diffusion-controlled drug release. Impressively, E/AC-Au/MTX not only significantly amplified the in vitro anticancer activity of MTX but also effectively suppressed tumor growth through oral administration. This led to a remarkable 60% reduction in tumor mass in mice bearing orthotopic HCT-116 tumors. These findings provide compelling evidence that E/AC-Au/MTX holds substantial promise as a specialized colonic drug delivery system designed to enhance the therapeutic outcomes of CRC. Furthermore, the adaptability of the AC-Au-based nanocomplex offers potential versatility, allowing its application to a diverse range of drugs. This extends its potential utility, opening new avenues in anticancer drug delivery.

## Data Sharing Statement

All data generated or analyzed during this study are included in this published article.

## Ethics Approval and Consent to Participate

All animal studies were approved by the review committee of Dongguk University (IACUC-2021-059-1).

## Funding

This research was supported by National Research Foundation of Korea (NRF) grant funded by the Korea government (MSIT) (Nos. 2019R1A2C2004873 and 2018R1A5A2023127) and the BK21 FOUR program through the National Research Foundation (NRF) funded by the Ministry of Education of Korea.

## Disclosure

The authors declare that they have no competing interests in this work.

## References

1. Perumal K, Ahmad S, Mohd-Zahid MH, et al. Nanoparticles and gut microbiota in colorectal cancer. *Front nanotechnol.* 2021;3:681760. doi:10.3389/fnano.2021.681760
2. Krasteva N, Georgieva M. Promising therapeutic strategies for colorectal cancer treatment based on nanomaterials. *Pharmaceutics.* 2022;14(6):1213. doi:10.3390/pharmaceutics14061213
3. Xie Y-H, Chen Y-X, Fang J-Y. Comprehensive review of targeted therapy for colorectal cancer. *Signal Transduct Target Ther.* 2020;5(1):22. doi:10.1038/s41392-020-0116-z
4. Tauriello DV, Calon A, Lonardo E, et al. Determinants of metastatic competency in colorectal cancer. *Mol Oncol.* 2017;11(1):97–119. doi:10.1002/1878-0261.12018
5. Gulbake A, Jain A, Jain A, et al. Insight to drug delivery aspects for colorectal cancer. *World J Gastroenterol.* 2016;22(2):582. doi:10.3748/wjg.v22.i2.582
6. Sahu BP, Baishya R, Hatiboruah JL, et al. A comprehensive review on different approaches for tumor targeting using nanocarriers and recent developments with special focus on multifunctional approaches. *J Pharm Investig.* 2022;52(5):539–585.

7. Bandi SP, Bhatnagar S, Venuganti VVK. Advanced materials for drug delivery across mucosal barriers. *Acta Biomater.* 2021;119:13–29. doi:10.1016/j.actbio.2020.10.031
8. Xu Y, Shrestha N, Pr  at V, et al. Overcoming the intestinal barrier: a look into targeting approaches for improved oral drug delivery systems. *J Control Release.* 2020;322:486–508. doi:10.1016/j.jconrel.2020.04.006
9. Elahi N, Kamali M, Baghersad MH. Recent biomedical applications of gold nanoparticles: a review. *Talanta.* 2018;184:537–556. doi:10.1016/j.talanta.2018.02.088
10. Beik J, Khateri M, Khosravi Z, et al. Gold nanoparticles in combinatorial cancer therapy strategies. *Coord Chem Rev.* 2019;387:299–324.
11. Anik MI, Mahmud N, Al Masud A, et al. Gold nanoparticles (GNPs) in biomedical and clinical applications: a review. *Nano Select.* 2022;3(4):792–828. doi:10.1002/nano.202100255
12. Lara P, Palma-Florez S, Salas-Huenuleo E, et al. Gold nanoparticle based double-labeling of melanoma extracellular vesicles to determine the specificity of uptake by cells and preferential accumulation in small metastatic lung tumors. *J Nanobiotechnology.* 2020;18(1):1–17. doi:10.1186/s12951-020-0573-0
13. Mohd-Zahid MH, Mohamud R, Abdullah CAC, et al. Colorectal cancer stem cells: a review of targeted drug delivery by gold nanoparticles. *RSC Adv.* 2020;10(2):973–985. doi:10.1039/C9RA08192E
14. Pal K, Al-Suraih F, Gonzalez-Rodriguez R, et al. Multifaceted peptide assisted one-pot synthesis of gold nanoparticles for plectin-1 targeted gemcitabine delivery in pancreatic cancer. *Nanoscale.* 2017;9(40):15622–15634. doi:10.1039/C7NR03172F
15. Amina SJ, Guo B. A review on the synthesis and functionalization of gold nanoparticles as a drug delivery vehicle. *Int J Nanomed.* 2020;2020:9823–9857.
16. Yang L, Shao Y, Han H-K. Aminoclay–lipid hybrid composite as a novel drug carrier of fenofibrate for the enhancement of drug release and oral absorption. *Int J Nanomed.* 2016;2016:1067–1076.
17. Kim S-Y, Lee S-J, Han H-K, et al. Aminoclay as a highly effective cationic vehicle for enhancing adenovirus-mediated gene transfer through nanobiohybrid complex formation. *Acta Biomater.* 2017;49:521–530. doi:10.1016/j.actbio.2016.11.045
18. Lee SH, Back S-Y, Song JG, et al. Enhanced oral delivery of insulin via the colon-targeted nanocomposite system of organoclay/glycol chitosan/Eudragit® S100. *J Nanobiotechnology.* 2020;18(1):1–10. doi:10.1186/s12951-020-00662-x
19. Park HJ, Lee SW, Song JG, et al. Aminoclay nanoparticles induce anti-inflammatory dendritic cells to attenuate LPS-elicited pro-inflammatory immune responses. *Molecules.* 2022;27(24):8743. doi:10.3390/molecules27248743
20. Hnatyszyn A, Hryhorowicz S, Kaczmarek-Rys M, et al. Colorectal carcinoma in the course of inflammatory bowel diseases. *Hered Cancer Clin Pract.* 2019;17(1):1–9. doi:10.1186/s13053-019-0118-4
21. Bui VKH, Park D, Lee Y-C. Aminoclays for biological and environmental applications: an updated review. *Chem Eng J.* 2018;336:757–772. doi:10.1016/j.cej.2017.12.052
22. Datta K, Eswaramoorthy M, Rao C. Water-solubilized aminoclay–metal nanoparticle composites and their novel properties. *J Mater Chem.* 2007;17(7):613–615. doi:10.1039/B617198B
23. Ravula S, Essner JB, La WA, et al. Sunlight-assisted route to antimicrobial plasmonic aminoclay catalysts. *Nanoscale.* 2015;7(1):86–91. doi:10.1039/C4NR04544K
24. Liao H-W, Hung M-C. Intracaeal orthotopic colorectal cancer xenograft mouse model. *Bio-protoc.* 2017;7(11):e2311. doi:10.21769/BioProtoc.2311
25. Song JG, Kim DH, Han H-K. Fabrication and evaluation of a pH-responsive nanocomposite-based colonic delivery system for improving the oral efficacy of liraglutide. *Int J Nanomedicine.* 2023;Volume 18:3937–3949. doi:10.2147/IJN.S413515
26. Lee Y-S, Song JG, Lee SH, et al. Sustained-release solid dispersion of pelubipofen using the blended mixture of aminoclay and pH independent polymers: preparation and in vitro / in vivo characterization. *Drug Deliv.* 2017;24(1):1731–1739. doi:10.1080/10717544.2017.1399304
27. Ahmed L, Atif R, Eldeen TS, et al. Study the using of nanoparticles as drug delivery system based on mathematical models for controlled release. *IJLTETAS.* 2019;8:52–56.
28. Akhter DT, Simpson JD, Fletcher NL, et al. Oral delivery of multicompartiment nanomedicines for colorectal cancer therapeutics: combining loco-regional delivery with cell-target specificity. *Adv Ther.* 2020;3(2):1900171. doi:10.1002/adtp.201900171
29. Chen Y-H, N-z X, Hong C, et al. Myo1b promotes tumor progression and angiogenesis by inhibiting autophagic degradation of HIF-1   in colorectal cancer. *Cell Death Dis.* 2022;13(11):939. doi:10.1038/s41419-022-05397-1
30.   lvarez-gonz  lez B, Rozalen M, Fern  ndez-Perales M, et al. Methotrexate gold nanocarriers: loading and release study: its activity in colon and lung cancer cells. *Molecules.* 2020;25(24):6049. doi:10.3390/molecules25246049
31. Manivasagan P, Bharathiraja S, Bui NQ, et al. Doxorubicin-loaded fucoidan capped gold nanoparticles for drug delivery and photoacoustic imaging. *Int J Biol Macromol.* 2016;91:578–588. doi:10.1016/j.ijbiomac.2016.06.007
32. Song JG, Lee SH, Han H-K. Development of an M cell targeted nanocomposite system for effective oral protein delivery: preparation, in vitro and in vivo characterization. *J Nanobiotechnology.* 2021;19:1–11. doi:10.1186/s12951-020-00750-y

## International Journal of Nanomedicine

Dovepress

## Publish your work in this journal

The International Journal of Nanomedicine is an international, peer-reviewed journal focusing on the application of nanotechnology in diagnostics, therapeutics, and drug delivery systems throughout the biomedical field. This journal is indexed on PubMed Central, MedLine, CAS, SciSearch®, Current Contents®/Clinical Medicine, Journal Citation Reports/Science Edition, EMBase, Scopus and the Elsevier Bibliographic databases. The manuscript management system is completely online and includes a very quick and fair peer-review system, which is all easy to use. Visit <http://www.dovepress.com/testimonials.php> to read real quotes from published authors.

Submit your manuscript here: <https://www.dovepress.com/international-journal-of-nanomedicine-journal>